

1 *Review*

# 2 **Recent insights from molecular dynamics simulations** 3 **for GPCR drug discovery**

4 **Ye Zou <sup>1</sup>, John Ewalt <sup>1</sup> and Ho-Leung Ng <sup>1,\*</sup>**

5 <sup>1</sup> Department of Biochemistry and Molecular Biophysics, Kansas State University, Manhattan, KS 66506, USA;  
6 [yezou@ksu.edu](mailto:yezou@ksu.edu) (Y. Z.); [ewalt@ksu.edu](mailto:ewalt@ksu.edu) (J. E.)

7 \* Correspondence: [hng@ksu.edu](mailto:hng@ksu.edu); Tel.: (+1-785-532-2518)

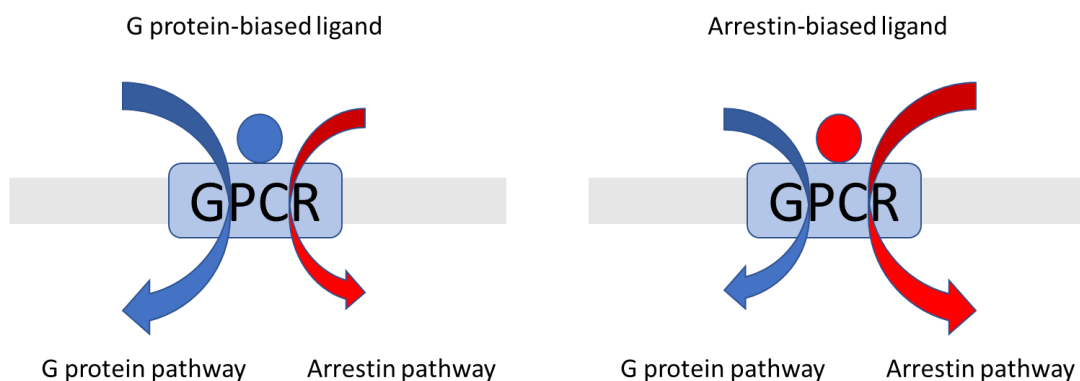
8  
9 **Abstract:** G protein-coupled receptors (GPCRs) are critical drug targets. GPCRs convey signals from the  
10 extracellular to the intracellular environment through G proteins. Some ligands that bind to GPCRs  
11 activate different downstream signaling pathways. G protein activation or  $\beta$ -arrestin biased signaling  
12 involves ligands binding to receptors and stabilizing conformations that trigger a specific pathway.  $\beta$ -  
13 arrestin biased signaling has become a hot target for structure-based drug discovery. However,  
14 challenges include that there are few crystal structures available in the Protein Data Bank and that  
15 GPCRs are highly dynamic. Hence, molecular dynamics (MD) simulations are especially valuable for  
16 obtaining detailed mechanistic information, including identification of allosteric sites and  
17 understanding modulators' interactions with receptors and ligands. Here, we highlight recent MD  
18 simulation studies and enhanced sampling methods used to study biased G protein-coupled receptor  
19 signaling and their conformational dynamics as well as applications to drug discovery.

20 **Keywords:** GPCRs; membrane protein; molecular dynamics; protein structure; drug design; biased-  
21 signaling pathway; allosteric sites  
22

## 23 **1. Introduction**

24 G protein-coupled receptors (GPCRs) are the largest superfamily of membrane proteins in the  
25 human genome [1]. They are also the most important and largest collection of pharmacological drug  
26 targets [2]. These receptors share modest sequence similarity but high structural conservation, all with  
27 seven transmembrane-spanning helices, an extracellular N terminus, and an intracellular C terminus.  
28 The crystal structure of bovine rhodopsin, one of the most studied GPCRs, shows the seven helices  
29 forming a helical cylinder, which is linked by three intracellular and three extracellular loops [3]. There  
30 are five main GPCR families: rhodopsin (class A), secretin (class B), glutamate (class C), frizzled/taste  
31 (class F), and adhesion [4]. GPCRs' typical functions are the translation of extracellular stimulation into  
32 intracellular signals via the binding of different ligands, which then cause different conformational  
33 changes and downstream effects. Each receptor can activate specific G proteins and regulate unique  
34 downstream signals. The GPCR ligands bind to these receptors and stabilize conformations, then  
35 regulate and modulate various intracellular transduction processes. GPCR agonist ligands are extremely  
36 diverse and include photons, ions, odorants, tastants, small molecule neurotransmitters, amino acids,  
37 polypeptides, hormones, nucleotides, and lipids [5, 6]. Classical GPCR activation involves an agonist-  
38 induced conformational change. This causes the receptor to interact with the  $G\alpha$  subunit, part of the  
39 heterotrimeric GTP-binding proteins (G proteins), which then dissociates from the  $G\beta\gamma$  subunits and  
40 binds to GDP. Research has also shown that there are also at least five different activation modes different  
41 from classical activations [7, 8]. These are involved in phenomena such as intracellular activation,  
42 dimerization activation, transactivation, biphasic activation, and biased activation. Because GPCRs are

43 involved in these activations, which are related to many human diseases, they are common drug targets  
 44 [9-12]. GPCRs are normally activated on the cell surface. GPCRs can also be activated from inside the cell,  
 45 which is called intracellular activation [13]. GPCR activation functions also depend on the forms of the  
 46 GPCRs, monomeric or dimeric, the latter of which is called dimerization activation [14]. GPCRs can be  
 47 activated by ligands and these activated GPCRs can transactivate other proteins, such as receptor tyrosine  
 48 kinases (RTKs), which then can activate Ras/MAP kinases. This is called transactivation [15]. GPCRs can  
 49 also activate two different phases of signaling. This is called biphasic activation [16]. The last activation  
 50 is called biased activation (Figure 1). The biased activation (also called biased signaling pathway)  
 51 involves parallel G protein-independent signaling pathways. Instead of activating G proteins, there are  
 52 activating  $\beta$ -arrestins, which mediate downstream signaling. The main functions are internalization and  
 53 desensitization. Activated by agonists, the GPCRs are phosphorylated by GPCR kinases (GRKs) on  
 54 multiple sites of the C-terminus, arrestins will bind to these phosphorylated sites, and G protein-coupling  
 55 will be blocked by the arrestin-GPCR complex. This is called biased activation [4, 17-20]. In this review  
 56 article, we focus on the biased-signaling pathway and  $\beta$ -arrestins. There are four classes of arrestins:  
 57 arrestin 1 (visual arrestin), arrestin 2 ( $\beta$ -arrestin 1), arrestin 3 ( $\beta$ -arrestin-2), and arrestin 4 (cone arrestin).  
 58 Arrestins are highly conserved, with approximately 50% sequence homology between vertebrates and  
 59 invertebrate primary structures [21-25]. Because the functions of arrestins are diverse,  $\beta$ -arrestin biased-  
 60 signaling pathways are of significant pharmaceutical interest. The current understanding of the  
 61 structural conformations related to biased signaling is sparse.  
 62



63  
 64  
 65 **Figure 1.** Overview of pathway-biased ligand activation for GPCRs  
 66  
 67

68 Recent studies have revealed that GPCRs are dynamic proteins with multiple conformational  
 69 changes depending on ligand binding, signaling proteins, and the membrane environment [26, 27].  
 70 Several crystals of class A GPCRs in the active state show there are conformational changes in the  
 71 intracellular domain and transmembrane helices 5, 6, 7 (TM5, TM6, and TM7) of the receptors [28-30].  
 72 Biophysical research has shown that the binding affinity to an agonist is increased by coupling the G  
 73 protein to the receptor [31]. After a ligand binds to a receptor, it causes and stabilizes conformational  
 74 changes [32]. Agonists binding to GPCRs induce and mediate different downstream pathways, either  
 75 through G protein activation or  $\beta$ -arrestin biased signaling. Typically, the primary ligand binding sites,  
 76 orthosteric sites, are highly conserved. This presents a significant challenge for drug discovery. Ideally,  
 77 a designed ligand has high selectivity and only activates specific receptors; an orthosteric site that is  
 78 highly conserved between related receptors increases the difficulty of doing so. Because of the challenges  
 79 these orthosteric sites present, researchers have been trying to explore new alternative binding sites,  
 80 which could increase both binding affinity and decrease off-target effects. Allosteric binding sites share  
 81 less homology compared to orthosteric sites, so they have become increasingly attractive to researchers

82 [33]. Positive allosteric modulators can increase the potency of orthosteric ligands; negative allosteric  
83 modulators can decrease the potency of the response to orthosteric ligands [34]. Several crystal structures  
84 of GPCRs bound with allosteric modulators have already been solved. Kruse et al. solved a crystal  
85 structure of a GPCR (M2 muscarinic receptor) with an allosteric modulator [30]. Dore et al. solved a class  
86 C GPCR (metabotropic glutamate receptor 5) bound with an allosteric modulator [35]. Jazayeri et al.  
87 solved a class B GPCR (glucagon receptor) bound with an allosteric antagonist [36]. However, it is also  
88 challenging to determine crystal structures of GPCRs with allosteric modulators, and few are in the PDB.  
89 Therefore, computational methods are valuable in helping to identify new allosteric binding sites and  
90 offer new structural information of GPCRs and their interactions with ligands.

91 Molecular dynamics simulations are important computational methods widely used in many fields  
92 of study. Simulations assist researchers in obtaining structural information, specifically, the  
93 conformational states that are hard to capture by experimental methods. Because of rapid technological  
94 development, computing is easier and faster than ever. This has also allowed researchers to run long time  
95 scale simulations to obtain more detailed mechanistic information [37]. In this review, we will discuss  
96 the insights on GPCR interactions with ligands revealed by molecular dynamics simulations and  
97 enhanced sampling techniques.

## 98 2. New insights from Molecular Dynamics Simulations

99 Computational and simulation methods provide other ways to explore complex systems which are  
100 difficult to study with current experimental methods. Simulation via molecular dynamics (MD) is a very  
101 powerful and easy to use computational tool. It can help researchers determine receptor-ligand structures,  
102 dynamics of binding, and binding kinetics and functions [38-41]. More recently, MD simulations have  
103 been used to study macromolecular conformational dynamics on longer time scales, up to a millisecond  
104 and beyond [42-45]. Computational and simulation methods can play useful roles in drug discovery as  
105 well. These methods have helped improve our understanding of GPCRs' structures and functions [2, 46-  
106 49]. There are three main requirements for an MD simulation: the model system, the force field, and the  
107 MD simulation software. The most popular MD simulation packages include AMBER [50], CHARMM  
108 [51], GROMACS [52], and NAMD [53]. These packages are making simulations easier to perform and are  
109 quick to adopt new technological and methodological advances.

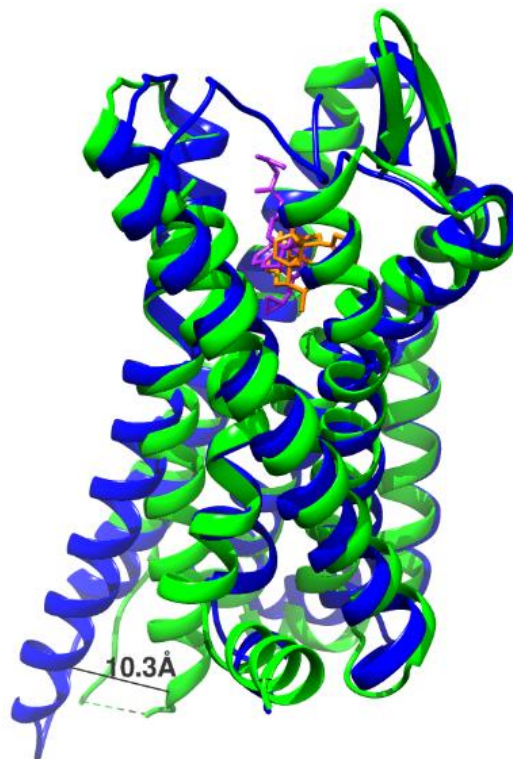
### 110 2.1. Using Molecular Dynamics Simulations to Study GPCR-Ligand Binding

111 Biased signaling generates functional selectivity and has attracted notable drug discovery interest.  
112 The structures and mechanisms involved in biased signaling are still not clear as there are very few GPCR  
113 crystal structures available.

114 The  $\mu$ -opioid receptor ( $\mu$ OR or MOR) is the first GPCR that demonstrated  $\beta$ -arrestin-biased signaling  
115 [54]. The  $\mu$ OR is the primary target for strong analgesics [55]. The best-known opioid agonists are opiate  
116 drugs, which are among the oldest medicines and are analgesics [56]. Even though opiates are widely  
117 used, they have notorious side effects including addiction, respiratory suppression, and constipation.  $\beta$ -  
118 arrestins act as negative regulators in the  $\mu$ OR signaling pathways [57, 58]. Recent research has supported  
119 a trend in which ligands that are more biased towards the  $\beta$ -arrestin pathway are associated with  
120 increased undesired side effects [59, 60]. Currently, there are two  $\mu$ OR crystal structures and two electron  
121 microscopy structures available in the Protein Data Bank (PDB: 4DKL, 5C1M, 6DDE/6DDF) [29, 61, 62].  
122 These high-resolution structures offer the possibilities of using these structures to perform simulations  
123 and potentially assist in the discovery of novel drugs with fewer side effects [9, 63, 64].

124 Crystallographic studies of  $\mu$ OR bound with the potent agonist, fentanyl, involved active and  
125 inactive states. The crystal structures used are PDB 5C1M and 4DKL. 4DKL is the structure of inactive  
126  $\mu$ OR with the irreversible morphinan antagonist  $\beta$ -funaltrexamine ( $\beta$ -FNA), which can be seen in Figure

127 2. 5C1M is the structure of active  $\mu$ OR with the agonist BU72. The primary structural difference between  
128 active and inactive states is TM6 shifting outwards by 10.3 Å [29].



129 **Figure 2.** Activation of  $\mu$ OR displaces TM6 by 10.3 Å. The inactive state is in blue and is bound to  
130 the antagonist  $\beta$ -FNA (purple). The active state is in green and is bound to the agonist BU72 (orange).  
131  
132  
133

134 Fentanyl is an analgesic that is much more potent and dangerous than morphine [65]. Unlike  
135 morphine, fentanyl can strongly induce  $\beta$ -arrestin biased signaling [66]. Both morphine and fentanyl  
136 have a protonatable tertiary amine in the piperidine ring. Compared to morphine, fentanyl is more  
137 flexible (Figure 3). Lipinski et al., using the 4DKL and 5C1M crystal structures and manually docking  
138 morphine and fentanyl into the protein, found that the mutation of Ser329<sup>7.46</sup> to alanine, located in the  
139 sodium binding pocket, is sensitive to the N-phenethyl chain of fentanyl [67]; mutations involving  
140 Trp318<sup>7.35</sup> and His319<sup>7.36</sup> to methionine demonstrate similar sensitivities to the N-phenethyl chain of  
141 fentanyl [68]. The superscript decimal numbers seen in the previous sentence refer to the Ballesteros-  
142 Weinstein numbering scheme, with the number to the left of the decimal referring to which of the 7  
143 transmembrane helices the residue is on and the number to the right of the decimal giving the relative  
144 position to the most conserved residue on the helix, which is numbered 50 [69].

145 In the fentanyl binding mode, both active and inactive receptors are stimulated. In the inactive mode,  
146 there is a sodium cation in an allosteric site. The simulation results of active and inactive binding  
147 interactions are similar. The two ligands both have the amine of the piperidine ring protonated. In the  
148 binding mode, the protonated amines interact with residue Asp147<sup>3.32</sup>; hence, the N-phenethyl chain is  
149 facing the intracellular side. The piperidine ring plays an important role in this binding mode. It interacts  
150 not only with A147<sup>3.32</sup> but also with Gln124<sup>2.60</sup>. The N-phenethyl chain forms hydrophobic contacts with  
151 Trp326<sup>7.43</sup>, Ile296<sup>6.51</sup>, Ile322<sup>7.39</sup>, and Trp293<sup>6.48</sup>. In the morphine binding mode, the simulation results of  
152 active and inactive binding interactions are also similar. The protonated amine in morphine also interacts  
153 with residue Asp147<sup>3.32</sup>. Morphine's binding pocket is similar to fentanyl's. The protonated amine is

154 facing intracellularly. The phenol and the ether group are facing the extracellular side and are exposed  
155 to the solvent. The CHARMM-GUI service [70] was used to parameterize and prepare the sample for  
156 simulation. The receptor was placed in a phosphatidylcholine (POPC) membrane and solvated with the  
157 TIP3P water model; the CHARMM36 force-field was used. The simulation runtime was 1.2  $\mu$ s [71].

158 In this research, MD simulations were also used to study a "Trp rotamer toggle switch" which acts  
159 as a transmission switch. Trp293<sup>6,48</sup> was found to be a highly conserved residue and multiple MD  
160 simulations support its central role in conformational change [72-74]. Analysis of MD simulations  
161 monitored the movement of Trp293<sup>6,48</sup> and focused on two different dihedral angles,  $\chi_1$  and  $\chi_2$ . Three  
162 rotamers were observed that differed from those seen in the crystal structure. Such rotamers would have  
163 been difficult to observe by experimental means.

164  
165



166

167 **Figure 3.** Chemical structures of  $\mu$ OR agonists: (a) morphine; (b) fentanyl.

168

## 169 2.2 Using Molecular Dynamics to Predict Arrestin-Biased Ligands

170 Pursuing biased signaling is an alternative strategy to discover highly selective drugs [75]. However,  
171 a detailed understanding of the biased signaling pathway is still incomplete. In particular, the crystal  
172 structures reported are of the active and inactive states, with very few structures that are relevant to  
173 intermediate conformations. MD simulations have assisted in revealing these intermediate  
174 conformations and the mechanisms of biased signaling. We discuss an example that used MD  
175 simulations to predict arrestin-biased ligands.

176 Recently, McCorvy et al. reported using the D2 dopamine receptor (D2R) as a model to study GPCR-  
177 ligand binding, which involves biased signaling, by MD simulations [76]. D2R is a primary drug target  
178 for schizophrenia and Parkinson's disease. The clinical implications of differently biased D2R ligands is  
179 a topic of great research interest. The authors describe a new method to use MD simulations to design  $\beta$ -  
180 arrestin biased ligands. The crystal structure of the complex of  $\beta_2$  adrenergic receptor ( $\beta_2$ AR) bound to  
181 epinephrine shows the ligand forms a hydrogen bond network with the conserved TM5 serine residues  
182 [77]. Three crystal structures of the GPCRs,  $\beta_2$ AR bound with epinephrine (4LDO), 5-HT<sub>2B</sub> serotonin  
183 receptor bound with lysergic acid diethylamide (LSD) (5TVN), and  $\beta_1$  adrenergic receptor ( $\beta_1$ AR) bound  
184 with 4-indole piperazine (3ZPQ), share conserved serine residues, 5.42, 5.43, and 5.46. The 5-HT<sub>2B</sub> crystal  
185 structure and MD simulations show that extracellular loop 2 (EL2) plays the role of a lid at the entrance  
186 to the binding pocket, slowing LSD's binding kinetics, which can be seen in Figure 4 [78].

187



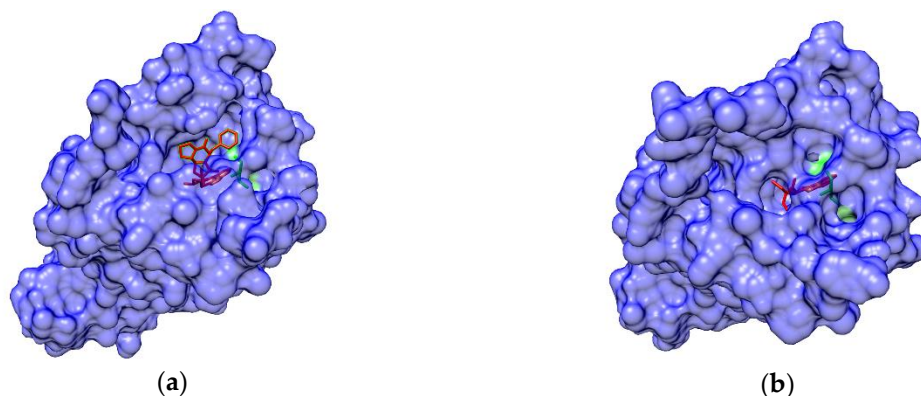


**Figure 4.** The binding pocket of 5-HT<sub>2B</sub> is (a) open when ergotamine binds and is (b) partially closed by movement of L209<sup>EL2</sup> when LSD binds.

There are conserved hydrophobic residues located in EL2, like isoleucine 184 (I184<sup>EL2</sup>) in D2R, which may lead to  $\beta$ -arrestin signaling in this receptor. They also did biophysical experiments to test the structure-functional selectivity relationships of the designed compounds such as indole N-substitutions. They were intended to disrupt interactions with TM5 and confirmed the validity of their simulations. MD simulations used a homology model based on the dopamine D3 receptor with the antagonist eticlopride (3PBL). MD simulations were used to predict EL2 engagement and find the key to biased signaling. The designed compounds contain an indole-piperazine moiety. The MD package AMBER14 was used. MD simulation results show that the conserved D114<sup>3,32</sup> forms a salt bridge with the protonated nitrogen piperazine ring in the orthosteric site. To better understand the mechanism between G protein activation and  $\beta$ -arrestin signaling, MD simulations were done without dihydroquinoline-2-one and the alkyl linker. These simulations showed that in the head group of compound 1 (Figure 5a), the hydrogen on the indole formed a hydrogen bond with S193<sup>5,42</sup> and did not interact with I184<sup>EL2</sup>. Instead of forming a hydrogen bond, the nitrogen on the indole of compound 2 was tracked by S193<sup>5,42</sup>; the center of the indole is closer to I184<sup>EL2</sup> than compound 1. The two compounds show different poses and interactions with GPCRs. Compound 1 is associated with G protein activation, and compound 2 (Figure 5b) is associated with  $\beta$ -arrestin biased signaling. Based on these critical simulation results, the authors were able to design new arrestin-biased compounds [76].

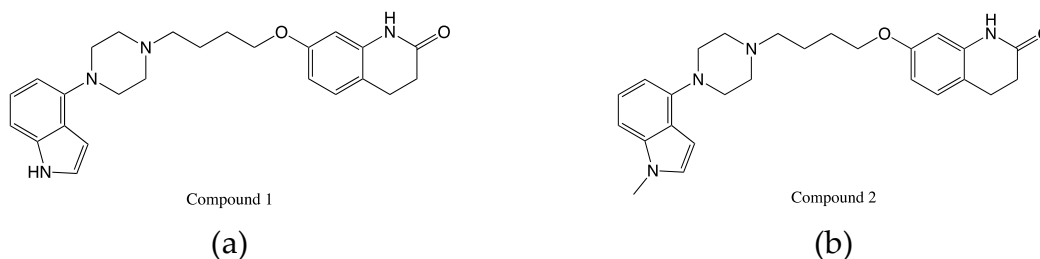
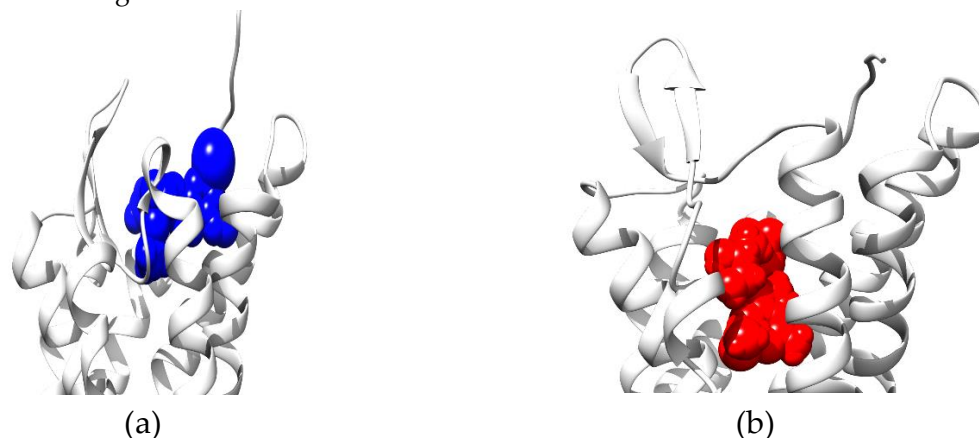


**Figure 5.** Structures of indole-aripiprazole hybrid compounds used to investigate D2R biased signaling: (a) compound 1; (b) compound 2 [76].

217 2.3 Identification of New Ligand Binding Sites and Activation Mechanisms by Accelerated Molecular Dynamics  
218 and Metadynamics Simulation

219 MD simulations have been commonly used to study GPCR activation mechanisms and  
220 conformational changes [79-81]. However, in the study of conformational dynamics, sampling the  
221 extended time-scales involved is the greatest challenge for MD simulation studies. To overcome this  
222 challenge, computational scientists have invented new methods and algorithms. Continued increases in  
223 computing power have also been of assistance. Currently, commonly used advanced hardware includes  
224 powerful graphics processing units (GPUs), supercomputers, and cloud computing [39, 82].  
225 Conventional molecular dynamics (cMD) simulations have been widely used to study GPCR activation  
226 mechanisms. cMD can reach timescales of microseconds [83-88]. However, there are many cases of GPCR  
227 activation processes that can take longer than the timescale limits of cMD simulation. Two of the most  
228 popular computational methods for enhanced sampling of protein molecular dynamics simulations to  
229 access longer time scales are accelerated molecular dynamics (aMD) and metadynamics [89]. aMD  
230 simulation improves conformational space sampling by adding a bias potential into cMD that reduces  
231 energy barriers between different states [90]. Metadynamics simulation parameterizes the model system  
232 with collective variables and introduces bias potentials to discourage resampling of explored  
233 conformational space [91]. As a result, both aMD and metadynamics simulations reduce calculation time  
234 and are much faster than regular cMD simulations at the risk of utilizing modified energy landscapes.  
235 Here, we discuss an example of using cMD and aMD simulations to find a new ligand-binding site and  
236 activation mechanism. P2Y<sub>1</sub>R is a purinergic GPCR that is activated by adenosine 5'-diphosphate (ADP).  
237 It plays an important role in platelet aggregation and thrombosis formation [92, 93]. The crystal structure  
238 of P2Y<sub>1</sub>R bound with the antagonist MRS2500 is available on Protein Data Bank (4XNW); however, there  
239 is no structure of P2Y<sub>1</sub>R bound with an agonist. Li et al. used cMD and aMD simulations to find a new  
240 agonist-binding site [94]. The crystal structure of P2Y<sub>1</sub>R bound with MRS2500 (4XNW), was used for  
241 simulation. The agonist, 2MeSADP, was docked to the same site as MRS2500. The results showed the  
242 aromatic adenine ring of 2MeSADP has a  $\pi$ - $\pi$  stacking interaction with Tyr303<sup>7,32</sup>. The pyrophosphates  
243 interact with Arg128<sup>3,29</sup> and Arg310<sup>7,39</sup>. However, these results did not match the experimental results.  
244 The experimental results show the mutagenesis of His132<sup>3,33</sup>, Tyr136<sup>3,37</sup>, and Lys280<sup>6,55</sup> decreased the  
245 binding affinity of 2MeSADP with P2Y<sub>1</sub>R. So, aMD simulations were used to run the long time-scale  
246 simulations necessary to find an alternative binding site, which can be seen in Figure 6. In this research,  
247 all MD simulations used the PMEMD (Particle Mesh Ewald Molecular Dynamics) module from  
248 AMBER14. The ff99SB force field was used for the receptor, and the general AMBER force field (GAFF)  
249 was used for the ligands.



250  
251  
252

253  
254  
255  
256  
257  
258  
259  
260  
261  
262  
263  
264  
  
265  
266  
267  
268  
269  
270  
271  
272  
273  
274  
275  
276  
277  
278  
279  
280  
281  
282  
283  
284  
285  
286  
287  
288  
289  
290  
291  
292  
293  
294  
295  
296  
297  
298

**Figure 6.** P2Y<sub>1</sub>R binding sites for (a) MRS2500 and (b) 2MeSADP.

The aMD simulations results show the aromatic adenine ring of 2MeSADP interacting with His132<sup>3.33</sup> through  $\pi$ - $\pi$  stacking interactions. The N<sup>1</sup> in the adenine forms hydrogen bonds with the Tyr136<sup>3.37</sup> and Thr221<sup>5.42</sup>. The pyrophosphates interact with Arg128<sup>3.29</sup>, Arg287<sup>6.62</sup>, Arg310<sup>7.39</sup>, Lys280<sup>6.55</sup>, and Tyr306<sup>7.35</sup>. These results match the experimental results. In this research, metadynamics simulations were used to obtain the potential of mean force for helices III-helix VI, which showed that 2MeSADP-P2Y<sub>1</sub>R has three states: inactive, intermediate, and active. Apo-P2Y<sub>1</sub>R and MRS2500-P2Y<sub>1</sub>R only have two states. The aMD simulation allowed 2MeSADP-P2Y<sub>1</sub>R to pass through the intermediate state and finally reach the active states from the inactive state [94].

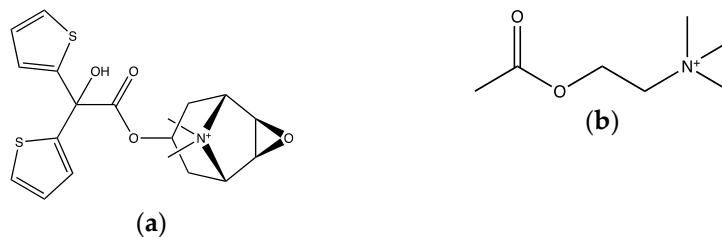
#### 2.4 Study of Allosteric Modulation and Dynamics of GPCR-Ligand Binding

Traditionally, research has focused on the orthosteric binding sites of GPCRs. There has been growing recent interest in allosteric sites especially regarding their advantages for drug discovery. Allosteric ligands can act as positive allosteric modulators, negative allosteric modulators, or neutral allosteric ligands. One of the advantages of allosteric modulators is that they have potentially better selectivity than orthosteric ligands [95].

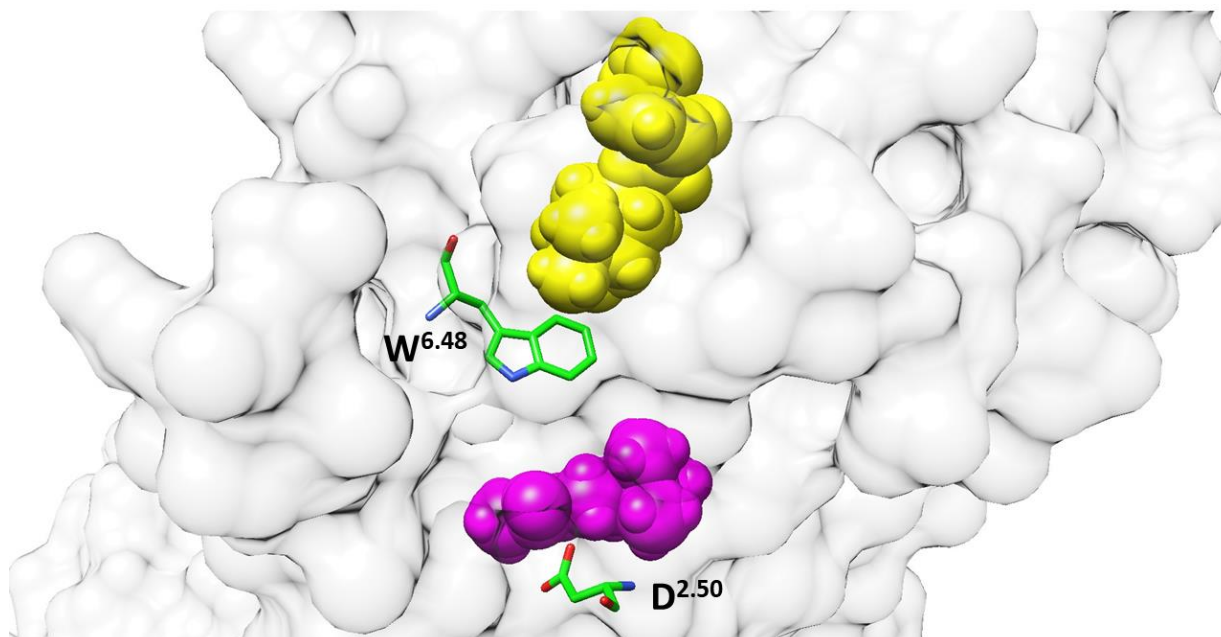
In studying the mechanisms of allosteric modulators, experiments such as x-ray crystallography, NMR, and systematic mutagenesis experiments have had important roles, and these techniques have already given researchers much conformational information of GPCRs and GPCR-mediated signaling. However, these methods only provide information on static conformational states, with the X-ray crystallography experiments only resolving two conformational states, active and inactive. There is no information about the conformations and transitions between these two states. The transition between inactive and active states is difficult to access by experimental methods. Currently, a more intricate, multi-state model, is being investigated by researchers [9, 96]. Molecular dynamics simulations give the possibility of revealing the intermediates of GPCRs between multiple states [9, 97, 98]. In the following section, we will discuss how molecular dynamics simulations provide information on intermediate states and can also identify new allosteric binding sites.

The muscarinic receptors are drug targets for many diseases such as overactive bladder, chronic obstructive pulmonary disease, and neurodegenerative diseases [99, 100]. Drug discovery for the muscarinic receptors has been hindered due to the challenge of selectively targeting receptor subtypes. The crystal structures of muscarinic M3 and M4 receptors show the antagonist tiotropium (TTP) in the orthosteric site (PDB: 4DAJ and 5DSG). The crystal structures show the orthosteric binding site is highly conserved [101, 102]. However, there is no crystal structure of a muscarinic receptor with agonist available yet. Chan et al. used MD simulations to simulate acetylcholine (ACh), the endogenous agonist, binding to M3 and M4 receptors [103]. Figure 7 shows the chemical structures of ACh and TTP. The simulation results show ACh binding to a new, deeper allosteric site near D<sup>2.50</sup> that is highly conserved [69]. To further understand the ACh activation process, an all-atom MD simulation was used to determine the ligand entrance pathway. ACh binds the orthosteric site, an aromatic cage, quickly (0.1-0.2  $\mu$ s). ACh was superimposed over TTP in the M3-TTP structure; both of their conformations are the same. After 0.5-0.6  $\mu$ s into the simulation, the ACh goes deeper into a new binding site and the pocket size is expanded. In contrast, during the entire simulation, TTP stays at the orthosteric site, as can be seen in Figure 8.





299 **Figure 7.** Chemical structures of muscarinic receptor ligands: (a) tiotropium (TTP); (b)  
 300 acetylcholine (ACh).



301 **Figure 8.** The M3 muscarinic receptor orthosteric binding site is near W<sup>6.48</sup> whereas the new  
 302 allosteric binding site is near D<sup>2.50</sup>.  
 303  
 304  
 305

306 The simulation also shows ACh interacting with residues A112<sup>2.57</sup>, I116<sup>2.53</sup>, A150<sup>3.35</sup>, S154<sup>3.39</sup>, and  
 307 W503<sup>6.48</sup>. In the M4 receptor MD simulation, ACh shows a similar binding behavior with the M3 receptor,  
 308 with ACh getting into a deeper binding site and next to D78<sup>2.50</sup>. The only difference is that there is an  
 309 ionic interaction between the quaternary nitrogen of ACh and D113<sup>2.50</sup>. In the M4-ACh model, the  
 310 quaternary nitrogen interacts with I81<sup>2.53</sup>, V115<sup>3.35</sup>, S116<sup>3.36</sup>, and S119<sup>3.39</sup>, because the ACh flips by 180  
 311 degrees.

312 MD simulations are also used to determine free energies. From the extracellular surface to the  
 313 orthosteric site to the new binding allosteric site, there are energy barriers between the orthosteric site  
 314 and the new binding site. This explains why ACh slowly moves from the orthosteric to the new binding  
 315 sites. These results demonstrate that molecular simulations can be used to determine free energy  
 316 differences between different binding states, which means that it can also potentially be used to design  
 317 new allosteric ligands.

318 In this research, the CHARRMM36 force field was used for the receptor and the CHARMM CgenFF  
 319 force field was used for the ligands. The MD package GROMACS was used. The simulation was run  
 320 longer than 3  $\mu$ s. Hence, these MD simulations have allowed researchers to see the entire process of ACh  
 321 binding to the orthosteric and allosteric sites. They also provided unique insights into mechanistic

322 differences induced by the agonist and antagonist. Both TTP and ACh have a quaternary nitrogen. The  
323 simulation results suggest that the positively charged nitrogen can be stabilized by forming ionic  
324 interactions with the highly conserved Asp<sup>250</sup> in both M3 and M4. This may help researchers identify and  
325 optimize future drug candidates. The successful identification of specific allosteric modulators for  
326 muscarinic receptors has already inspired similar approaches targeting other receptors involved in  
327 neurodegenerative and psychiatric diseases [104].

328 An interesting interaction between a positively charged ligand nitrogen atom and a negatively  
329 charged receptor aspartate is also observed in the simulation studies of  $\mu$ OR. The two opioid ligands,  
330 fentanyl and morphine, both have a protonated nitrogen amine in the piperidine ring. Both interact with  
331 Asp147<sup>3,32</sup>. In M3 and M4, the positive nitrogen charges form interactions with Asp<sup>250</sup>. The positive  
332 nitrogen charges in the ligands apparently plays a central role in binding and activation.

### 333 3. Insights of Molecular Dynamics to Drug Design

334 Drug discovery is among the most challenging of scientific enterprises: it is high risk, high cost, and  
335 requires a long time to move from the bench to the market [105]. Early-stage structure-based drug design  
336 has the potential to de-risk and accelerate projects. The recent, tremendous advances in GPCR  
337 crystallography have provided new opportunities for structure-based drug design [106-109]. Increasing  
338 experimental evidence shows that the GPCR-signaling pathway is more complicated than classical  
339 signaling [11]. The multiple mechanisms of GPCR activation and regulation offer diverse possibilities for  
340 drug discovery [110, 111].

341 GPCRs undergo major conformational changes during their functional cycles. Researchers  
342 frequently want to design a ligand that can specifically bind to the target, in addition to wanting the  
343 ligand to activate or inactivate a desired signaling pathway with little to no off-target effects. To reach  
344 this point, the designed ligand needs to bind to a specific binding site so that it induces certain  
345 conformational states of the receptor. Therefore, understanding the structural dynamics and the  
346 mechanisms of various signaling pathways of GPCRs is crucial to the design of GPCR-targeted ligands.  
347 As described above, GPCR functional mechanisms are extremely complicated. Hence, understanding  
348 receptor dynamics is very important for drug design. There is growing interest in using allosteric  
349 modulators for GPCR drug discovery [112]. It has been difficult thus far to identify new allosteric binding  
350 sites from crystal structures, in the rare cases that crystal structures are even available. MD simulations  
351 can help researchers solve these problems.

352 Enhanced sampling methods play an important role in this research. Adaptive biased techniques  
353 offer the chance to shorten simulation time, thus decreasing computational cost, and lets ligands explore  
354 more conformational space by making it easier to escape local minima. aMD, one of the more popular  
355 adaptive-biased methods, allows the dynamic processes that are required to have agonists pass some  
356 energy barriers and reach new energy states. This should allow the possibility of finding new allosteric  
357 sites. Metadynamics allows researchers to observe the 2D energy landscape, thus easily seeing the energy  
358 differences in all the states. They can serve as a reliability check on the results that aMD provides [94]. To  
359 achieve these enhanced sampling methods, the most popular MD packages currently available include  
360 Amber, NAMD, GROMACS, and CHARMM. To obtain an accurate result, the force field chosen plays a  
361 very important role. The ff99SB and ff14SB force fields are those most commonly used with Amber.  
362 ff14SB is similar to ff99SB; however, ff14SB was modified by empirical adjustments of the protein  
363 backbone dihedral parameters,  $\phi$  and  $\psi$  [113]. CHARMM36 is a force field commonly used with NAMD  
364 and CHARMM, which includes improved refined backbone CMAP (a grid-based correction for the  $\phi$ -  
365  $\psi$ -angular dependence of the energy) potentials and side-chain dihedral parameters [114]. To obtain new  
366 and accurate insights from simulations, the inclusion of lipids in the model system is important.  
367 Experimental results show that bovine rhodopsin is sensitive to lipid environments [115, 116]. Crozier et  
368 al. are the first to report computational insight about rhodopsin-lipid interactions [117]. They found

369 differences of lipid accessibility differences for the transmembrane helices of rhodopsin. Later, Lyman et  
370 al. reported the adenosine A<sub>2A</sub> receptor in a cholesterol-free POPC membrane, both with and without the  
371 antagonist ZM241385. It showed that there is a gap between TM1 and TM2, which allows the lipid  
372 headgroup into the binding site and causes receptor instability when there is no ligand present. This  
373 prediction was proved later [118]. This is also a good example of long-time scale simulation, with the  
374 time scale being 3  $\mu$ s. Simulations with longer time scales may give us new insights on slower developing  
375 phenomena. Previously, simulations performed by Lipinski et al. were longer than 1.2  $\mu$ s, from which  
376 the “Trp rotamer toggle switch” was found.

377 The primary goal when designing a GPCR-targeted drug is normally to make a ligand that, in  
378 addition to binding the desired target, also creates a specific signaling profile. To achieve the desired  
379 signaling profile, the drug needs to be able to stabilize certain conformational states of the receptor. If the  
380 desired conformational change involves an agonist creating more stabilized active states compared to  
381 inactive states, something that needs to be taken into account is how minor changes in the structure of  
382 the binding pocket can be associated with different signaling profiles and different intracellular coupling  
383 interface conformations [9]. There are challenges involved in successfully doing this. Small changes in  
384 one area of the binding pocket can have larger effects elsewhere in the pocket. Changes in an area  
385 completely outside of the pocket itself can also have small or large effects throughout the pocket, and  
386 vice versa: the latter of which can be important when an allosteric modulator is introduced after the  
387 orthosteric ligand is already in the orthosteric binding site. Further difficulties can arise if one seeks to  
388 design a modulator that only affects arrestin signaling when changes to any of the sites mentioned above  
389 can have an effect on G protein and/or arrestin signaling [9].

390 The potential contributions of simulations include helping identify important interactions the  
391 orthosteric ligand can make with the binding pocket or rearrangements of the binding pocket induced  
392 by the ligand. They can also assist with characterizing receptor pocket dynamics, both for known  
393 structures based on experiments as well as intermediate or metastable states that are difficult or  
394 impossible to currently access experimentally. Another potential use is assessing how ligands affect the  
395 pocket and receptor dynamics, and comparing dynamics of closely related GPCRs, which should allow  
396 more precise and specific ligand design [9].

397 A simulation-based approach was used to design chemical modifications that substantially altered  
398 a modulator’s allosteric effects on the M2 muscarinic receptor. The modulators the researchers initially  
399 studied all partially block the ingress and egress of orthosteric ligands. The allosteric binding site is along  
400 the path that the orthosteric ligands take to binding to the orthosteric site, which is curious because the  
401 modulators studied also weakened the association and dissociation of the orthosteric ligands.  
402 Simulations indicated that the ligand interaction mode was different than initially proposed. The  
403 researchers were able to design new modulators that took advantage of information about ligand  
404 interactions from the simulation results: the measured affinities of the new modulators were consistent  
405 with that predicted by the simulations [43].

#### 406 4. Summary and Perspectives

407 Computational methods are essential tools for biomacromolecular structural studies. GPCRs are the  
408 largest class of drug targets and have structural flexibility, dynamic structures, and complex biological  
409 functions. Recent breakthroughs in GPCR crystallography have enabled accurate and predictive MD  
410 simulations. Here, we have reviewed recent works that have used MD simulations and enhanced  
411 sampling methods to study interactions with new ligands, characterize unknown active/inactive states,  
412 and identify new binding sites. This has allowed researchers to gain insights to study new potential drug  
413 candidates and obtain qualitative structural information with less time. With computers and algorithms  
414 continually growing faster, computational methods will be even more effective in helping future  
415 researchers reveal the inner mysteries of GPCRs and their ligands.

416 The ever-increasing number of GPCR structures found by molecular dynamics simulations of crystal  
417 structures will provide a growing database from which new ligands and potentially new binding sites  
418 can be determined and explored. Because testing *in silico* is less resource intensive than *in vitro* or *in vivo*,  
419 this should allow researchers to find new interesting drug targets.

420 **Funding:** This research was funded by National Science Foundation CAREER Award MCB 1833181.

421 **Conflicts of Interest:** The authors declare no conflict of interest.

## 422 Abbreviations

GPCR	G protein-coupled receptor
GDP	Guanosine diphosphate
RTKs	receptor tyrosine kinases
MAP	Mitogen-activated protein
GRKs	GPCR kinases
$\mu$ OR/MOR	$\mu$ -opioid receptor
MD	Molecular dynamics
cMD	Conventional molecular dynamics
aMD	Accelerated molecular dynamics
PMEMD	Particle Mesh Ewald Molecular Dynamics
GAFF	General AMBER force field
PDB	Protein Data Bank
ACh	Acetylcholine
POPC	Phosphatidylcholine
TTP	Tiotropium
SBDD	Structure-based drug design

423

424



425 **References**

- 426 1. Rosenbaum, D. M.; Rasmussen, S. G.; Kobilka, B. K., The structure and function of G-protein-  
427 coupled receptors. *Nature* **2009**, 459, (7245), 356.
- 428 2. Hauser, A. S.; Attwood, M. M.; Rask-Andersen, M.; Schioth, H. B.; Gloriam, D. E., Trends in  
429 GPCR drug discovery: new agents, targets and indications. *Nat Rev Drug Discov* **2017**, 16, (12),  
430 829-842.
- 431 3. Palczewski, K.; Kumasaka, T.; Hori, T.; Behnke, C. A.; Motoshima, H.; Fox, B. A.; Le Trong, I.;  
432 Teller, D. C.; Okada, T.; Stenkamp, R. E., Crystal structure of rhodopsin: A G protein-coupled  
433 receptor. *Science* **2000**, 289, (5480), 739-745.
- 434 4. Alexander, S. P.; Davenport, A. P.; Kelly, E.; Marrion, N.; Peters, J. A.; Benson, H. E.; Faccenda,  
435 E.; Pawson, A. J.; Sharman, J. L.; Southan, C., The Concise Guide to PHARMACOLOGY 2015/16:  
436 G protein-coupled receptors. *British journal of pharmacology* **2015**, 172, (24), 5744-5869.
- 437 5. Allen, J. A.; Roth, B. L., Strategies to discover unexpected targets for drugs active at G protein-  
438 coupled receptors. *Annu Rev Pharmacol Toxicol* **2011**, 51, 117-44.
- 439 6. Roth, B. L.; Kroeze, W. K., Integrated Approaches for Genome-wide Interrogation of the  
440 Druggable Non-olfactory G Protein-coupled Receptor Superfamily. *J Biol Chem* **2015**, 290, (32),  
441 19471-7.
- 442 7. Wang, W.; Qiao, Y.; Li, Z., New Insights into Modes of GPCR Activation. *Trends Pharmacol Sci*  
443 **2018**, 39, (4), 367-386.
- 444 8. Zhou, X. E.; Melcher, K.; Xu, H. E., Understanding the GPCR biased signaling through G protein  
445 and arrestin complex structures. *Curr Opin Struct Biol* **2017**, 45, 150-159.
- 446 9. Latorraca, N. R.; Venkatakrisnan, A. J.; Dror, R. O., GPCR Dynamics: Structures in Motion. *Chem*  
447 *Rev* **2017**, 117, (1), 139-155.
- 448 10. Lee, Y.; Lazim, R.; Macalino, S. J. Y.; Choi, S., Importance of protein dynamics in the structure-  
449 based drug discovery of class A G protein-coupled receptors (GPCRs). *Curr Opin Struct Biol* **2019**,  
450 55, 147-153.
- 451 11. Wacker, D.; Stevens, R. C.; Roth, B. L., How Ligands Illuminate GPCR Molecular Pharmacology.  
452 *Cell* **2017**, 170, (3), 414-427.
- 453 12. Kaczor, A. A.; Rutkowska, E.; Bartuzi, D.; Targowska-Duda, K. M.; Matosiuk, D.; Selent, J.,  
454 Computational methods for studying G protein-coupled receptors (GPCRs). *Methods Cell Biol*  
455 **2016**, 132, 359-99.
- 456 13. Schiaffino, M. V.; d'Addio, M.; Alloni, A.; Baschiroto, C.; Valetti, C.; Cortese, K.; Puri, C.; Bassi,  
457 M. T.; Colla, C.; De Luca, M., Ocular albinism: evidence for a defect in an intracellular signal  
458 transduction system. *Nature genetics* **1999**, 23, (1), 108.
- 459 14. Gomes, I.; Jordan, B. A.; Gupta, A.; Rios, C.; Trapaidze, N.; Devi, L. A., G protein coupled receptor  
460 dimerization: implications in modulating receptor function. *Journal of molecular medicine* **2001**, 79,  
461 (5-6), 226-242.
- 462 15. Daub, H.; Weiss, F. U.; Wallasch, C.; Ullrich, A., Role of transactivation of the EGF receptor in  
463 signalling by G-protein-coupled receptors. *Nature* **1996**, 379, (6565), 557.

- 464 16. Schorb, W.; Conrad, K. M.; Singer, H. A.; Dostal, D. E.; Baker, K. M., Angiotensin II is a potent  
465 stimulator of MAP-kinase activity in neonatal rat cardiac fibroblasts. *Journal of molecular and*  
466 *cellular cardiology* **1995**, 27, (5), 1151-1160.
- 467 17. DeWire, S. M.; Ahn, S.; Lefkowitz, R. J.; Shenoy, S. K., Beta-arrestins and cell signaling. *Annu Rev*  
468 *Physiol* **2007**, 69, 483-510.
- 469 18. Lefkowitz, R. J., Historical review: a brief history and personal retrospective of seven-  
470 transmembrane receptors. *Trends Pharmacol Sci* **2004**, 25, (8), 413-22.
- 471 19. Milligan, G.; Kostenis, E., Heterotrimeric G-proteins: a short history. *Br J Pharmacol* **2006**, 147  
472 Suppl 1, S46-55.
- 473 20. Scheerer, P.; Sommer, M. E., Structural mechanism of arrestin activation. *Curr Opin Struct Biol*  
474 **2017**, 45, 160-169.
- 475 21. Attramadal, H.; Arriza, J. L.; Aoki, C.; Dawson, T. M.; Codina, J.; Kwatra, M. M.; Snyder, S. H.;  
476 Caron, M. G.; Lefkowitz, R. J., Beta-arrestin 2, a novel member of the arrestin/beta-arrestin gene  
477 family. *Journal of Biological Chemistry* **1992**, 267, (25), 17882-17890.
- 478 22. Benovic, J.; Kühn, H.; Weyand, I.; Codina, J.; Caron, M.; Lefkowitz, R., Functional desensitization  
479 of the isolated beta-adrenergic receptor by the beta-adrenergic receptor kinase: potential role of  
480 an analog of the retinal protein arrestin (48-kDa protein). *Proceedings of the National Academy of*  
481 *Sciences* **1987**, 84, (24), 8879-8882.
- 482 23. Craft, C. M.; Whitmore, D. H.; Wiechmann, A. F., Cone arrestin identified by targeting expression  
483 of a functional family. *Journal of Biological Chemistry* **1994**, 269, (6), 4613-4619.
- 484 24. Gainetdinov, R. R.; Premont, R. T.; Bohn, L. M.; Lefkowitz, R. J.; Caron, M. G., Desensitization of  
485 G protein-coupled receptors and neuronal functions. *Annu Rev Neurosci* **2004**, 27, 107-44.
- 486 25. Smith, J. S.; Rajagopal, S., The beta-Arrestins: Multifunctional Regulators of G Protein-coupled  
487 Receptors. *J Biol Chem* **2016**, 291, (17), 8969-77.
- 488 26. Nygaard, R.; Zou, Y.; Dror, R. O.; Mildorf, T. J.; Arlow, D. H.; Manglik, A.; Pan, A. C.; Liu, C. W.;  
489 Fung, J. J.; Bokoch, M. P.; Thian, F. S.; Kobilka, T. S.; Shaw, D. E.; Mueller, L.; Prosser, R. S.;  
490 Kobilka, B. K., The dynamic process of beta2-adrenergic receptor activation. *Cell* **2013**, 152, (3),  
491 532-42.
- 492 27. Vaidehi, N.; Bhattacharya, S., Allosteric communication pipelines in G-protein-coupled receptors.  
493 *Current opinion in pharmacology* **2016**, 30, 76-83.
- 494 28. Burg, J. S.; Ingram, J. R.; Venkatakrishnan, A.; Jude, K. M.; Dukkupati, A.; Feinberg, E. N.;  
495 Angelini, A.; Waghray, D.; Dror, R. O.; Ploegh, H. L., Structural basis for chemokine recognition  
496 and activation of a viral G protein-coupled receptor. *Science* **2015**, 347, (6226), 1113-1117.
- 497 29. Huang, W.; Manglik, A.; Venkatakrishnan, A. J.; Laeremans, T.; Feinberg, E. N.; Sanborn, A. L.;  
498 Kato, H. E.; Livingston, K. E.; Thorsen, T. S.; Kling, R. C.; Granier, S.; Gmeiner, P.; Husbands, S.  
499 M.; Traynor, J. R.; Weis, W. I.; Steyaert, J.; Dror, R. O.; Kobilka, B. K., Structural insights into mu-  
500 opioid receptor activation. *Nature* **2015**, 524, (7565), 315-21.
- 501 30. Kruse, A. C.; Ring, A. M.; Manglik, A.; Hu, J.; Hu, K.; Eitel, K.; Hübner, H.; Pardon, E.; Valant, C.;  
502 Sexton, P. M., Activation and allosteric modulation of a muscarinic acetylcholine receptor. *Nature*  
503 **2013**, 504, (7478), 101.

- 504 31. Yao, X. J.; Velez Ruiz, G.; Whorton, M. R.; Rasmussen, S. G. F.; DeVree, B. T.; Deupi, X.; Sunahara,  
505 R. K.; Kobilka, B., The effect of ligand efficacy on the formation and stability of a GPCR-G protein  
506 complex. *Proceedings of the National Academy of Sciences* **2009**, 106, (23), 9501-9506.
- 507 32. Vaidehi, N.; Kenakin, T., The role of conformational ensembles of seven transmembrane  
508 receptors in functional selectivity. *Current opinion in pharmacology* **2010**, 10, (6), 775-781.
- 509 33. Christopoulos, A., Advances in G protein-coupled receptor allostery: from function to structure.  
510 *Mol Pharmacol* **2014**, 86, (5), 463-78.
- 511 34. Foster, D. J.; Conn, P. J., Allosteric Modulation of GPCRs: New Insights and Potential Utility for  
512 Treatment of Schizophrenia and Other CNS Disorders. *Neuron* **2017**, 94, (3), 431-446.
- 513 35. Dore, A. S.; Okrasa, K.; Patel, J. C.; Serrano-Vega, M.; Bennett, K.; Cooke, R. M.; Errey, J. C.;  
514 Jazayeri, A.; Khan, S.; Tehan, B.; Weir, M.; Wiggin, G. R.; Marshall, F. H., Structure of class C  
515 GPCR metabotropic glutamate receptor 5 transmembrane domain. *Nature* **2014**, 511, (7511), 557-  
516 62.
- 517 36. Jazayeri, A.; Dore, A. S.; Lamb, D.; Krishnamurthy, H.; Southall, S. M.; Baig, A. H.; Bortolato, A.;  
518 Koglin, M.; Robertson, N. J.; Errey, J. C.; Andrews, S. P.; Teobald, I.; Brown, A. J.; Cooke, R. M.;  
519 Weir, M.; Marshall, F. H., Extra-helical binding site of a glucagon receptor antagonist. *Nature*  
520 **2016**, 533, (7602), 274-7.
- 521 37. Karplus, M.; McCammon, J. A., Molecular dynamics simulations of biomolecules. *Nature*  
522 *Structural & Molecular Biology* **2002**, 9, (9), 646.
- 523 38. Cournia, Z.; Allen, T. W.; Andricioaei, I.; Antonny, B.; Baum, D.; Brannigan, G.; Buchete, N.-V.;  
524 Deckman, J. T.; Delemotte, L.; Del Val, C., Membrane protein structure, function, and dynamics:  
525 a perspective from experiments and theory. *The Journal of membrane biology* **2015**, 248, (4), 611-640.
- 526 39. Dror, R. O.; Dirks, R. M.; Grossman, J.; Xu, H.; Shaw, D. E., Biomolecular simulation: a  
527 computational microscope for molecular biology. *Annual review of biophysics* **2012**, 41, 429-452.
- 528 40. Khalili-Araghi, F.; Gumbart, J.; Wen, P.-C.; Sotomayor, M.; Tajkhorshid, E.; Schulten, K.,  
529 Molecular dynamics simulations of membrane channels and transporters. *Current opinion in*  
530 *structural biology* **2009**, 19, (2), 128-137.
- 531 41. Stansfeld, P. J.; Sansom, M. S., Molecular simulation approaches to membrane proteins. *Structure*  
532 **2011**, 19, (11), 1562-1572.
- 533 42. Dror, R. O.; Arlow, D. H.; Borhani, D. W.; Jensen, M. Ø.; Piana, S.; Shaw, D. E., Identification of  
534 two distinct inactive conformations of the  $\beta_2$ -adrenergic receptor reconciles structural and  
535 biochemical observations. *Proceedings of the National Academy of Sciences* **2009**, 106, (12), 4689-4694.
- 536 43. Dror, R. O.; Green, H. F.; Valant, C.; Borhani, D. W.; Valcourt, J. R.; Pan, A. C.; Arlow, D. H.;  
537 Canals, M.; Lane, J. R.; Rahmani, R., Structural basis for modulation of a G-protein-coupled  
538 receptor by allosteric drugs. *Nature* **2013**, 503, (7475), 295.
- 539 44. Grossfield, A.; Pitman, M. C.; Feller, S. E.; Soubias, O.; Gawrisch, K., Internal hydration increases  
540 during activation of the G-protein-coupled receptor rhodopsin. *Journal of molecular biology* **2008**,  
541 381, (2), 478-486.

- 542 45. Gumbart, J. C.; Teo, I.; Roux, B.; Schulten, K., Reconciling the roles of kinetic and thermodynamic  
543 factors in membrane–protein insertion. *Journal of the American Chemical Society* **2013**, *135*, (6), 2291-  
544 2297.
- 545 46. De Vivo, M.; Masetti, M.; Bottegoni, G.; Cavalli, A., Role of Molecular Dynamics and Related  
546 Methods in Drug Discovery. *J Med Chem* **2016**, *59*, (9), 4035-61.
- 547 47. Dror, R. O.; Pan, A. C.; Arlow, D. H.; Borhani, D. W.; Maragakis, P.; Shan, Y.; Xu, H.; Shaw, D. E.,  
548 Pathway and mechanism of drug binding to G-protein-coupled receptors. *Proc Natl Acad Sci U S*  
549 *A* **2011**, *108*, (32), 13118-23.
- 550 48. Marino, K. A.; Filizola, M., Investigating small-molecule ligand binding to G protein-coupled  
551 receptors with biased or unbiased molecular dynamics simulations. In *Computational Methods for*  
552 *GPCR Drug Discovery*, Springer: 2018; pp 351-364.
- 553 49. Sabbadin, D.; Moro, S., Supervised molecular dynamics (SuMD) as a helpful tool to depict GPCR-  
554 ligand recognition pathway in a nanosecond time scale. *J Chem Inf Model* **2014**, *54*, (2), 372-6.
- 555 50. Case, D.; Ben-Shalom, I.; Brozell, S.; Cerutti, D.; Cheatham III, T.; Cruzeiro, V.; Darden, T.; Duke,  
556 R.; Ghoreishi, D.; Gilson, M., AMBER 2018; 2018. *University of California, San Francisco*.
- 557 51. Brooks, B. R.; Bruccoleri, R. E.; Olafson, B. D.; States, D. J.; Swaminathan, S. a.; Karplus, M.,  
558 CHARMM: a program for macromolecular energy, minimization, and dynamics calculations.  
559 *Journal of computational chemistry* **1983**, *4*, (2), 187-217.
- 560 52. Hess, B.; Kutzner, C.; Van Der Spoel, D.; Lindahl, E., GROMACS 4: algorithms for highly efficient,  
561 load-balanced, and scalable molecular simulation. *Journal of chemical theory and computation* **2008**,  
562 *4*, (3), 435-447.
- 563 53. Phillips, J. C.; Braun, R.; Wang, W.; Gumbart, J.; Tajkhorshid, E.; Villa, E.; Chipot, C.; Skeel, R. D.;  
564 Kale, L.; Schulten, K., Scalable molecular dynamics with NAMD. *Journal of computational*  
565 *chemistry* **2005**, *26*, (16), 1781-1802.
- 566 54. Violin, J. D.; Lefkowitz, R. J., Beta-arrestin-biased ligands at seven-transmembrane receptors.  
567 *Trends Pharmacol Sci* **2007**, *28*, (8), 416-22.
- 568 55. Vardanyan, R. S.; Hruby, V. J., Fentanyl-related compounds and derivatives: current status and  
569 future prospects for pharmaceutical applications. *Future medicinal chemistry* **2014**, *6*, (4), 385-412.
- 570 56. Stein, C., Opioid receptors. *Annual review of medicine* **2016**, *67*, 433-451.
- 571 57. Pasternak, G. W.; Pan, Y. X., Mu opioids and their receptors: evolution of a concept. *Pharmacol*  
572 *Rev* **2013**, *65*, (4), 1257-317.
- 573 58. Raehal, K. M.; Bohn, L. M., Mu opioid receptor regulation and opiate responsiveness. *The AAPS*  
574 *journal* **2005**, *7*, (3), E587-E591.
- 575 59. Conibear, A. E.; Kelly, E., A biased view of mu opioid receptors? *Mol Pharmacol* **2019**.
- 576 60. Schmid, C. L.; Kennedy, N. M.; Ross, N. C.; Lovell, K. M.; Yue, Z.; Morgenweck, J.; Cameron, M.  
577 D.; Bannister, T. D.; Bohn, L. M., Bias Factor and Therapeutic Window Correlate to Predict Safer  
578 Opioid Analgesics. *Cell* **2017**, *171*, (5), 1165-1175 e13.
- 579 61. Koehl, A.; Hu, H.; Maeda, S.; Zhang, Y.; Qu, Q.; Paggi, J. M.; Latorraca, N. R.; Hilger, D.; Dawson,  
580 R.; Matile, H.; Schertler, G. F. X.; Granier, S.; Weis, W. I.; Dror, R. O.; Manglik, A.; Skiniotis, G.;



- 581 Kobilka, B. K., Structure of the mu-opioid receptor-Gi protein complex. *Nature* **2018**, 558, (7711),  
582 547-552.
- 583 62. Manglik, A.; Kruse, A. C.; Kobilka, T. S.; Thian, F. S.; Mathiesen, J. M.; Sunahara, R. K.; Pardo, L.;  
584 Weis, W. I.; Kobilka, B. K.; Granier, S., Crystal structure of the mu-opioid receptor bound to a  
585 morphinan antagonist. *Nature* **2012**, 485, (7398), 321-6.
- 586 63. Kaserer, T.; Lantero, A.; Schmidhammer, H.; Spetea, M.; Schuster, D., mu Opioid receptor: novel  
587 antagonists and structural modeling. *Sci Rep* **2016**, 6, 21548.
- 588 64. Manglik, A.; Lin, H.; Aryal, D. K.; McCorvy, J. D.; Dengler, D.; Corder, G.; Levit, A.; Kling, R. C.;  
589 Bernat, V.; Hubner, H.; Huang, X. P.; Sassano, M. F.; Giguere, P. M.; Lober, S.; Da, D.; Scherrer,  
590 G.; Kobilka, B. K.; Gmeiner, P.; Roth, B. L.; Shoichet, B. K., Structure-based discovery of opioid  
591 analgesics with reduced side effects. *Nature* **2016**, 537, (7619), 185-190.
- 592 65. Bremer, P. T.; Kimishima, A.; Schlosburg, J. E.; Zhou, B.; Collins, K. C.; Janda, K. D., Combatting  
593 Synthetic Designer Opioids: A Conjugate Vaccine Ablates Lethal Doses of Fentanyl Class Drugs.  
594 *Angewandte Chemie International Edition* **2016**, 55, (11), 3772-3775.
- 595 66. Zheng, H.; Chu, J.; Zhang, Y.; Loh, H. H.; Law, P. Y., Modulating mu-opioid receptor  
596 phosphorylation switches agonist-dependent signaling as reflected in PKCepsilon activation and  
597 dendritic spine stability. *J Biol Chem* **2011**, 286, (14), 12724-33.
- 598 67. Pil, J.; Tytgat, J., Serine 329 of the mu-opioid receptor interacts differently with agonists. *J*  
599 *Pharmacol Exp Ther* **2003**, 304, (3), 924-30.
- 600 68. Ulens, C.; Van Boven, M.; Daenens, P.; Tytgat, J., Interaction of p-fluorofentanyl on cloned human  
601 opioid receptors and exploration of the role of Trp-318 and His-319 in  $\mu$ -opioid receptor  
602 selectivity. *Journal of Pharmacology and Experimental Therapeutics* **2000**, 294, (3), 1024-1033.
- 603 69. Isberg, V.; de Graaf, C.; Bortolato, A.; Cherezov, V.; Katritch, V.; Marshall, F. H.; Mordalski, S.;  
604 Pin, J. P.; Stevens, R. C.; Vriend, G.; Gloriam, D. E., Generic GPCR residue numbers - aligning  
605 topology maps while minding the gaps. *Trends Pharmacol Sci* **2015**, 36, (1), 22-31.
- 606 70. Jo, S.; Kim, T.; Iyer, V. G.; Im, W., CHARMM-GUI: a web-based graphical user interface for  
607 CHARMM. *J Comput Chem* **2008**, 29, (11), 1859-65.
- 608 71. Lipinski, P. F. J.; Jaronczyk, M.; Dobrowolski, J. C.; Sadlej, J., Molecular dynamics of fentanyl  
609 bound to mu-opioid receptor. *J Mol Model* **2019**, 25, (5), 144.
- 610 72. Marino, K. A.; Shang, Y.; Filizola, M., Insights into the function of opioid receptors from  
611 molecular dynamics simulations of available crystal structures. *British journal of pharmacology*  
612 **2018**, 175, (14), 2834-2845.
- 613 73. Shang, Y.; LeRouzic, V.; Schneider, S.; Bisignano, P.; Pasternak, G. W.; Filizola, M., Mechanistic  
614 insights into the allosteric modulation of opioid receptors by sodium ions. *Biochemistry* **2014**, 53,  
615 (31), 5140-5149.
- 616 74. Sutcliffe, K. J.; Henderson, G.; Kelly, E.; Sessions, R. B., Drug binding poses relate structure with  
617 efficacy in the  $\mu$  opioid receptor. *Journal of molecular biology* **2017**, 429, (12), 1840-1851.
- 618 75. Soergel, D. G.; Subach, R. A.; Burnham, N.; Lark, M. W.; James, I. E.; Sadler, B. M.; Skobieranda,  
619 F.; Violin, J. D.; Webster, L. R., Biased agonism of the  $\mu$ -opioid receptor by TRV130 increases

- analgesia and reduces on-target adverse effects versus morphine: a randomized, double-blind, placebo-controlled, crossover study in healthy volunteers. *PAIN* **2014**, *155*, (9), 1829-1835.
- 622 76. McCorvy, J. D.; Butler, K. V.; Kelly, B.; Rechsteiner, K.; Karpiak, J.; Betz, R. M.; Kormos, B. L.;  
623 Shoichet, B. K.; Dror, R. O.; Jin, J.; Roth, B. L., Structure-inspired design of beta-arrestin-biased  
624 ligands for aminergic GPCRs. *Nat Chem Biol* **2018**, *14*, (2), 126-134.
- 625 77. Ring, A. M.; Manglik, A.; Kruse, A. C.; Enos, M. D.; Weis, W. I.; Garcia, K. C.; Kobilka, B. K.,  
626 Adrenaline-activated structure of  $\beta$ 2-adrenoceptor stabilized by an engineered nanobody. *Nature*  
627 **2013**, *502*, (7472), 575.
- 628 78. Wacker, D.; Wang, S.; McCorvy, J. D.; Betz, R. M.; Venkatakrisnan, A.; Levit, A.; Lansu, K.;  
629 Schools, Z. L.; Che, T.; Nichols, D. E., Crystal structure of an LSD-bound human serotonin  
630 receptor. *Cell* **2017**, *168*, (3), 377-389. e12.
- 631 79. Dror, R. O.; Arlow, D. H.; Maragakis, P.; Mildorf, T. J.; Pan, A. C.; Xu, H.; Borhani, D. W.; Shaw,  
632 D. E., Activation mechanism of the  $\beta$ 2-adrenergic receptor. *Proceedings of the National Academy of*  
633 *Sciences* **2011**, *108*, (46), 18684-18689.
- 634 80. Esguerra, M.; Siretskiy, A.; Bello, X.; Sallander, J.; Gutiérrez-de-Terán, H., GPCR-ModSim: A  
635 comprehensive web based solution for modeling G-protein coupled receptors. *Nucleic acids*  
636 *research* **2016**, *44*, (W1), W455-W462.
- 637 81. Zeng, L.; Guan, M.; Jin, H.; Liu, Z.; Zhang, L., Integrating Pharmacophore into Membrane  
638 Molecular Dynamics Simulations to Improve Homology Modeling of G Protein-coupled  
639 Receptors with Ligand Selectivity: A2A Adenosine Receptor as an Example. *Chemical biology &*  
640 *drug design* **2015**, *86*, (6), 1438-1450.
- 641 82. Kohlhoff, K. J.; Shukla, D.; Lawrenz, M.; Bowman, G. R.; Konerding, D. E.; Belov, D.; Altman, R.  
642 B.; Pande, V. S., Cloud-based simulations on Google Exacycle reveal ligand modulation of GPCR  
643 activation pathways. *Nature chemistry* **2014**, *6*, (1), 15.
- 644 83. Bai, Q.; Shi, D.; Zhang, Y.; Liu, H.; Yao, X., Exploration of the antagonist CP-376395 escape  
645 pathway for the corticotropin-releasing factor receptor 1 by random acceleration molecular  
646 dynamics simulations. *Molecular BioSystems* **2014**, *10*, (7), 1958-1967.
- 647 84. Shukla, D.; Hernández, C. X.; Weber, J. K.; Pande, V. S., Markov state models provide insights  
648 into dynamic modulation of protein function. *Accounts of chemical research* **2015**, *48*, (2), 414-422.
- 649 85. Vaidehi, N.; Bhattacharya, S.; Larsen, A. B., Structure and dynamics of G-protein coupled  
650 receptors. In *G Protein-Coupled Receptors-Modeling and Simulation*, Springer: 2014; pp 37-54.
- 651 86. Xiao, X.; Zeng, X.; Yuan, Y.; Gao, N.; Guo, Y.; Pu, X.; Li, M., Understanding the conformation  
652 transition in the activation pathway of  $\beta$ 2 adrenergic receptor via a targeted molecular dynamics  
653 simulation. *Physical Chemistry Chemical Physics* **2015**, *17*, (4), 2512-2522.
- 654 87. Xu, J.; Wang, Z.; Liu, P.; Li, D.; Lin, J., An insight into antagonist binding and induced  
655 conformational dynamics of class B GPCR corticotropin-releasing factor receptor 1. *Molecular*  
656 *BioSystems* **2015**, *11*, (7), 2042-2050.
- 657 88. Yang, L.; Yang, D.; De Graaf, C.; Moeller, A.; West, G. M.; Dharmarajan, V.; Wang, C.; Siu, F. Y.;  
658 Song, G.; Reedtz-Runge, S., Conformational states of the full-length glucagon receptor. *Nature*  
659 *communications* **2015**, *6*, 7859.

- 660 89. Maximova, T.; Moffatt, R.; Ma, B.; Nussinov, R.; Shehu, A., Principles and Overview of Sampling  
661 Methods for Modeling Macromolecular Structure and Dynamics. *PLoS Comput Biol* **2016**, *12*, (4),  
662 e1004619.
- 663 90. Hamelberg, D.; Mongan, J.; McCammon, J. A., Accelerated molecular dynamics: a promising and  
664 efficient simulation method for biomolecules. *The Journal of chemical physics* **2004**, *120*, (24), 11919-  
665 11929.
- 666 91. Valsson, O.; Tiwary, P.; Parrinello, M., Enhancing Important Fluctuations: Rare Events and  
667 Metadynamics from a Conceptual Viewpoint. *Annu Rev Phys Chem* **2016**, *67*, 159-84.
- 668 92. Gachet, C., P2 receptors, platelet function and pharmacological implications. *Thrombosis and*  
669 *haemostasis* **2008**, *99*, (03), 466-472.
- 670 93. Jacobson, K. A.; Deflorian, F.; Mishra, S.; Costanzi, S., Pharmacochimistry of the platelet  
671 purinergic receptors. *Purinergic signalling* **2011**, *7*, (3), 305-324.
- 672 94. Li, Y.; Yin, C.; Liu, P.; Li, D.; Lin, J., Identification of a Different Agonist-Binding Site and  
673 Activation Mechanism of the Human P2Y 1 Receptor. *Scientific reports* **2017**, *7*, (1), 13764.
- 674 95. Wootten, D.; Christopoulos, A.; Sexton, P. M., Emerging paradigms in GPCR allostery:  
675 implications for drug discovery. *Nat Rev Drug Discov* **2013**, *12*, (8), 630-44.
- 676 96. Bar-Shavit, R.; Maoz, M.; Kancharla, A.; Nag, J. K.; Agranovich, D.; Grisaru-Granovsky, S.; Uziely,  
677 B., G Protein-Coupled Receptors in Cancer. *Int J Mol Sci* **2016**, *17*, (8).
- 678 97. Rajagopal, S.; Rajagopal, K.; Lefkowitz, R. J., Teaching old receptors new tricks: biasing seven-  
679 transmembrane receptors. *Nat Rev Drug Discov* **2010**, *9*, (5), 373-86.
- 680 98. Violin, J. D.; Crombie, A. L.; Soergel, D. G.; Lark, M. W., Biased ligands at G-protein-coupled  
681 receptors: promise and progress. *Trends Pharmacol Sci* **2014**, *35*, (7), 308-16.
- 682 99. Felder, C. C.; Goldsmith, P. J.; Jackson, K.; Sanger, H. E.; Evans, D. A.; Mogg, A. J.; Broad, L. M.,  
683 Current status of muscarinic M1 and M4 receptors as drug targets for neurodegenerative diseases.  
684 *Neuropharmacology* **2018**, *136*, (Pt C), 449-458.
- 685 100. Kruse, A. C.; Kobilka, B. K.; Gautam, D.; Sexton, P. M.; Christopoulos, A.; Wess, J., Muscarinic  
686 acetylcholine receptors: novel opportunities for drug development. *Nat Rev Drug Discov* **2014**, *13*,  
687 (7), 549-60.
- 688 101. Kruse, A. C.; Hu, J.; Pan, A. C.; Arlow, D. H.; Rosenbaum, D. M.; Rosemond, E.; Green, H. F.; Liu,  
689 T.; Chae, P. S.; Dror, R. O.; Shaw, D. E.; Weis, W. I.; Wess, J.; Kobilka, B. K., Structure and  
690 dynamics of the M3 muscarinic acetylcholine receptor. *Nature* **2012**, *482*, (7386), 552-6.
- 691 102. Thal, D. M.; Sun, B.; Feng, D.; Nawaratne, V.; Leach, K.; Felder, C. C.; Bures, M. G.; Evans, D. A.;  
692 Weis, W. I.; Bachhawat, P.; Kobilka, T. S.; Sexton, P. M.; Kobilka, B. K.; Christopoulos, A., Crystal  
693 structures of the M1 and M4 muscarinic acetylcholine receptors. *Nature* **2016**, *531*, (7594), 335-40.
- 694 103. Chan, H. C. S.; Wang, J.; Palczewski, K.; Filipek, S.; Vogel, H.; Liu, Z. J.; Yuan, S., Exploring a new  
695 ligand binding site of G protein-coupled receptors. *Chem Sci* **2018**, *9*, (31), 6480-6489.
- 696 104. Bock, A.; Schrage, R.; Mohr, K., Allosteric modulators targeting CNS muscarinic receptors.  
697 *Neuropharmacology* **2018**, *136*, (Pt C), 427-437.

- 698 105. Paul, S. M.; Mytelka, D. S.; Dunwiddie, C. T.; Persinger, C. C.; Munos, B. H.; Lindborg, S. R.;  
699 Schacht, A. L., How to improve R&D productivity: the pharmaceutical industry's grand  
700 challenge. *Nat Rev Drug Discov* **2010**, 9, (3), 203-14.
- 701 106. Jazayeri, A.; Dias, J. M.; Marshall, F. H., From G Protein-coupled Receptor Structure Resolution  
702 to Rational Drug Design. *J Biol Chem* **2015**, 290, (32), 19489-95.
- 703 107. Kooistra, A. J.; Leurs, R.; De Esch, I. J.; de Graaf, C., From three-dimensional GPCR structure to  
704 rational ligand discovery. In *G Protein-Coupled Receptors-Modeling and Simulation*, Springer: 2014;  
705 pp 129-157.
- 706 108. Kumari, P.; Ghosh, E.; Shukla, A. K., Emerging Approaches to GPCR Ligand Screening for Drug  
707 Discovery. *Trends Mol Med* **2015**, 21, (11), 687-701.
- 708 109. Shoichet, B. K.; Kobilka, B. K., Structure-based drug screening for G-protein-coupled receptors.  
709 *Trends Pharmacol Sci* **2012**, 33, (5), 268-72.
- 710 110. Kaya, C.; Armutlulu, A.; Ekesan, S.; Haliloglu, T., MCPPath: Monte Carlo path generation  
711 approach to predict likely allosteric pathways and functional residues. *Nucleic Acids Res* **2013**, 41,  
712 (Web Server issue), W249-55.
- 713 111. Marti-Solano, M.; Kaczor, A. A.; Guixà-González, R.; Selent, J., Computational Strategies to  
714 Incorporate GPCR Complexity in Drug Design. In *Frontiers in Computational Chemistry*, Elsevier:  
715 2015; pp 3-43.
- 716 112. Huang, X.-P.; Karpiak, J.; Kroeze, W. K.; Zhu, H.; Chen, X.; Moy, S. S.; Sadoris, K. A.; Nikolova,  
717 V. D.; Farrell, M. S.; Wang, S., Allosteric ligands for the pharmacologically dark receptors GPR68  
718 and GPR65. *Nature* **2015**, 527, (7579), 477.
- 719 113. Maier, J. A.; Martinez, C.; Kasavajhala, K.; Wickstrom, L.; Hauser, K. E.; Simmerling, C., ff14SB:  
720 Improving the Accuracy of Protein Side Chain and Backbone Parameters from ff99SB. *J Chem*  
721 *Theory Comput* **2015**, 11, (8), 3696-713.
- 722 114. Huang, J.; MacKerell, A. D., Jr., CHARMM36 all-atom additive protein force field: validation  
723 based on comparison to NMR data. *J Comput Chem* **2013**, 34, (25), 2135-45.
- 724 115. Soubias, O.; Teague, W. E., Jr.; Hines, K. G.; Mitchell, D. C.; Gawrisch, K., Contribution of  
725 membrane elastic energy to rhodopsin function. *Biophys J* **2010**, 99, (3), 817-24.
- 726 116. Zaitseva, E.; Brown, M. F.; Vogel, R., Sequential rearrangement of interhelical networks upon  
727 rhodopsin activation in membranes: the Meta II(a) conformational substate. *J Am Chem Soc* **2010**,  
728 132, (13), 4815-21.
- 729 117. Crozier, P. S.; Stevens, M. J.; Forrest, L. R.; Woolf, T. B., Molecular dynamics simulation of dark-  
730 adapted rhodopsin in an explicit membrane bilayer: coupling between local retinal and larger  
731 scale conformational change. *J Mol Biol* **2003**, 333, (3), 493-514.
- 732 118. Hanson, M. A.; Cherezov, V.; Griffith, M. T.; Roth, C. B.; Jaakola, V. P.; Chien, E. Y.; Velasquez,  
733 J.; Kuhn, P.; Stevens, R. C., A specific cholesterol binding site is established by the 2.8 Å structure  
734 of the human beta2-adrenergic receptor. *Structure* **2008**, 16, (6), 897-905.
- 735